Effects of $m \neq 0$ Tip States in Scanning Tunneling Microscopy: The Explanations of Corrugation Reversal

C. Julian Chen

IBM Thomas J. Watson Research Center, P.O. Box 218, Yorktown Heights, New York 10598

(Received 22 June 1992)

We analyze the effects of $m \neq 0$ tip states in scanning tunneling microscopy (STM). If near the Fermi level, an $m \neq 0$ tip state dominates, images with large but *inverted* atomic corrugation are expected. This provides an explanation of the STM images with inverted corrugations, and the sudden reversal of the STM corrugation from inverted to noninverted. An analysis of the effects of various combinations of $m \neq 0$ and $m = 0$ d-type tip states is presented. We show that in most cases, a stable and large corrugation enhancement, either positive or negative, is expected, with predicted values in agreement with experimental observations.

PACS numbers: 61.16.Di, 61.50.Em

On the images of clean metal surfaces obtained by the scanning tunneling microscope (STM), in many cases, the sites of metal atoms are minima rather than maxima [1]. This phenomenon, the *inverted corrugation* or the *negative images*, has been the topic of a number of theoretical studies [2,3]. In an extensive experimental STM study of the Au(111) surface [4], some of the best atom-resolved images are actually negative. The absolute values of the corrugation amplitudes for the negative images can be a large fraction of an angstrom, an order of magnitude greater than what is expected from the charge density contour. It is also reported that with a sudden change of the tip, under the same tunneling conditions, the STM image switches abruptly from negative to positive. Such a spontaneous reversal of corrugation indicates that it is a tip-state effect, not a sample-state effect [4]. Furthermore, while the atomic corrugation is inverted, the average contour of the large reconstruction remains unchanged [4].

In a previous Letter [5], we show that with an $l = 2$, $m = 0$ (i.e., d_{z^2}) tip state, the atomic corrugation of the STM image of metal surfaces can be more than 1 order of magnitude greater than the corrugation of the Fermi-level local density of states (LDOS), which provides an explanation of the experimentally observed atomic resolution on metal surfaces [6]. In this case, the image is positive, i.e., the atomic sites appear as protrusions in the topographic images [5,6]. In general, on various surfaces of d-band metals, such as W, Pt, or Ir, the electronic states with different m have comparable probability to dominate the Fermi-level DOS. Slab calculations [7] showed that on the W(001) surface, at the Fermi level, d states with different m occupy different regions in the first surface Brillouin zone. Although near the $\bar{\Gamma}$ point, the d_{z^2} state dominates the Fermi-level LDOS [8], on irregular surfaces such as various STM tips, the $m \neq 0$ states have a sizable probability to dominate the Fermi-level DOS. A cluster calculation [9] reached a similar conclusion. On the apex of a W_4 cluster, the highest occupied molecular orbital (HOMO) is a d_{z^2} state, whereas the lowest unoccupied molecular orbital (LUMO) is an $m \neq 0$ state. On the other hand, on the apex of a W_5 cluster, the HOMO is an $m \neq 0$ state, whereas the LUMO is a d_{z^2} state. Therefore, depending on the surrounding atomic structure of the tip, either state can dominate the Fermi-level LDOS. Here, we show that when an $m \neq 0$ state dominates the tip LDOS near the Fermi level, the STM image should exhibit a large but *inverted* atomic corrugation; and hence a minor change in the tip structure may cause a corrugation reversal.

First, we present a qualitative explanation of the effect of $m \neq 0$ tip states in the light of the reciprocity principle [5]. The tunneling current is symmetric regarding the tip state and the sample state. Figure 1 shows the LDOS of various kinds of tip states at a plane $z_0 = 3$ Å from the nucleus of the apex atom. The LDOS is normalized over the plane. For simplicity, we assume that the tip has an axial symmetry. In other words, the two $m = 1$ states, xz and yz, are degenerate. Similarly, the two $m = 2$ states, xy and $x^2 - y^2$, are also degenerate. Following Tersoff

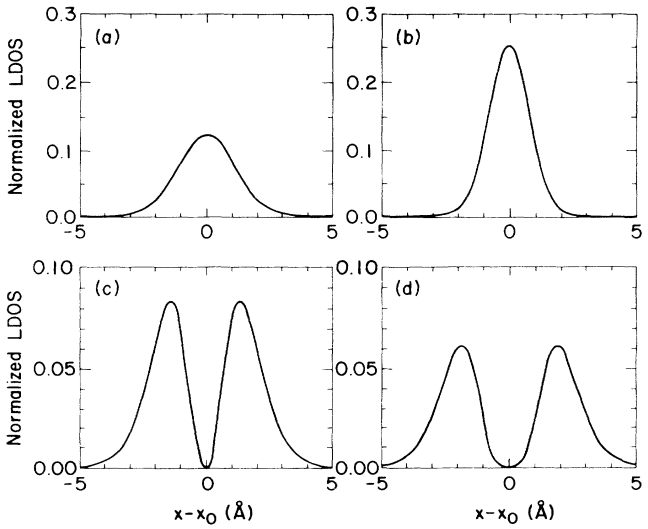

FIG. 1. LDOS of several tip electronic states, evaluated and normalized on a plane $z_0 = 3$ Å from the nucleus of the apex atom. An axial symmetry is assumed. (a) s state. (b) $l = 2$, $m = 0$ state ($d_{3z^2-r^2}$). (c) $l = 2$, $m = 1$ states (d_{xz} and d_{yz}). (d) $l = 2$, $m = 2$ states ($d_{x^2-y^2}$ and d_{xy}).

TABLE I. Wave functions and tunneling matrix elements for d tip states. The tip is assumed to have an axial symmetry, and the coefficients for the two $m=1$ states are the same. Similarly, the coefficients for the two $m=2$ states are the same. For brevity, the common factor in the normalization constant of the spherical harmonics and a common factor $2\pi\hbar^2/\kappa m_e$ in the expressions for the tunneling matrices are omitted.

m	Component	Tip wave function	Tunneling matrix element
0	$3z^2-r^2$	$D_0 k_2(\kappa r)[3\cos^2\theta-1]$	$D_0[3\kappa^{-2}\partial^2/\partial z^2-1]\psi(\mathbf{r}_0)$
1	xz	$D_1 k_2(\kappa r)\sqrt{3}\sin 2\theta\cos\phi$	$D_1[2\sqrt{3}\kappa^{-2}\partial^2/\partial x\partial z]\psi(\mathbf{r}_0)$
1	yz	$D_1 k_2(\kappa r)\sqrt{3}\sin 2\theta\sin\phi$	$D_1[2\sqrt{3}\kappa^{-2}\partial^2/\partial y\partial z]\psi(\mathbf{r}_0)$
2	x^2-y^2	$D_2 k_2(\kappa r)\sqrt{3}\sin^2\theta\cos 2\phi$	$D_2[\sqrt{3}\kappa^{-2}(\partial^2/\partial x^2-\partial^2/\partial y^2)]\psi(\mathbf{r}_0)$
2	xy	$D_2 k_2(\kappa r)\sqrt{3}\sin^2\theta\sin 2\phi$	$D_2[2\sqrt{3}\kappa^{-2}\partial^2/\partial x\partial y]\psi(\mathbf{r}_0)$

and Hamann [10], we assume that the method of atomic charge superposition is valid for describing the LDOS of the gold surface. Each Au atom at the surface has only s-wave states near the Fermi level. Then, according to the s-wave tip theory of STM [10], the tunneling current distribution between a single Au atom and the tip is the tip-state LDOS, measured at the center of that Au atom. For a d_{z^2} tip state [see Fig. 1(b)], it has a sharp peak centered at the atom site. The total current distribution is the sum of tunneling current for all the Au atoms at the surface. The sharpness of the tunneling current distribution for the d_{z^2} tip state, compared with that of the s-wave tip state [Fig. 1(a)], again illustrates why the d_{z^2} tip state enhances image corrugation [5]. The $m=1$ and $m=2$ tip states exhibit a ring-shaped LDOS, as shown in Figs. 1(c) and 1(d). According to the s-wave tip theory of STM [10], the tunneling current distribution for a single Au atom should be proportional to the tip LDOS, which is ring shaped [Figs. 1(c) and 1(d)]. The total current distribution is the sum of the tunneling current for all the Au atoms at the surface. Therefore, with an $m\neq 0$ tip state, an inverted STM image should be expected. In other words, every site of Au atom at the surface should appear as a depression rather than a protrusion in the STM image.

In the following, we present a quantitative analysis of the STM image corrugation by considering various combinations of d-type states. For clarity, we confine our discussions for the tips with an axial symmetry. We illustrate it with a hexagonal-close-packed metal surface, using the method described previously [5,11]. The vacuum tails of the five d states and the corresponding tunneling matrix elements are listed in Table I. The degeneracy due to axial symmetry of the tip is reflected in the choice of coefficients. Those coefficients, D_0, D_1, and D_2, depend strongly on the specific structure of the tip, and can be predicted by first-principles calculations [7–9]. The leading term of the surface Bloch wave near the $\bar{\Gamma}$ point is (see Fig. 2 in Ref. [5])

$$\psi_0 = B_0 \exp(-\kappa z)\,, \tag{1}$$

where the decay constant κ is determined by the work function ϕ through the relation $\kappa=(2m_e\phi)^{1/2}/\hbar \simeq 0.51\sqrt{\phi}$, in Å and eV. B_0 is a constant, to be determined later. The leading Fourier components of the Bloch waves at the six $\bar{K}$ points are [5] (see Fig. 2 in Ref. [5])

$$\psi_1 = B_1 \exp(-\kappa_1 z)\sum_{j=0}^{2}\exp(ik_1\boldsymbol{\Omega}_j\cdot\mathbf{x})\,, \tag{2}$$

and its complex conjugate. Here, $\boldsymbol{\Omega}_0=(1,0)$, $\boldsymbol{\Omega}_1=(-\frac{1}{2},\frac{1}{2}\sqrt{3})$, $\boldsymbol{\Omega}_2=(-\frac{1}{2},-\frac{1}{2}\sqrt{3})$ are unit vectors on the (x,y) plane, $k_1=4\pi/3a$ is the magnitude of the Bloch vector at the $\bar{K}$ points, and $\kappa_1=[\kappa^2+k_1^2]^{1/2}$ is the corresponding decay constant. B_1 is another constant to be determined later.

The general expression for the tunneling current can be obtained using the explicit forms of tunneling matrix elements [11], listed in Table I. Up to a constant, the tunneling current is

$$I = 4|D_0B_0|^2 e^{-2\kappa z} + 9|D_0B_1|^2 e^{-2\kappa_1 z}[3(\kappa_1/\kappa)^2-1]^2\phi^{(6)}(k\mathbf{x}) + 54|D_1B_1|^2 e^{-2\kappa_1 z}(k_1\kappa_1/\kappa^2)^2[1-\phi^{(6)}(k\mathbf{x})] + \tfrac{27}{2}|D_2B_1|^2 e^{-2\kappa_1 z}(k_1/\kappa)^4[1-\phi^{(6)}(k\mathbf{x})]\,. \tag{3}$$

The hexagonal cosine function $\phi^{(6)}(k\mathbf{x})$ is defined as [5]

$$\phi^{(6)}(\mathbf{X}) \equiv \frac{1}{3}+\frac{2}{9}\sum_{j=0}^{2}\cos\boldsymbol{\omega}_j\cdot\mathbf{X}\,, \tag{4}$$

where $\boldsymbol{\omega}_0=(0,1)$, $\boldsymbol{\omega}_1=(-\frac{1}{2}\sqrt{3},-\frac{1}{2})$, and $\boldsymbol{\omega}_2=(\frac{1}{2}\sqrt{3},-\frac{1}{2})$, respectively. The quantity k is the length of the primitive reciprocal-lattice vector, $k=4\pi/\sqrt{3}a$, and $\mathbf{x}\equiv(x,y)$ (see Fig. 2 in Ref. [5]). The function $\phi^{(6)}(k\mathbf{x})$ has maximum value 1 at each atomic site, and nearly zero between atoms which describes a positive corrugation. The function $1-\phi^{(6)}(k\mathbf{x})$ thus has a minimum 0 at each atomic site, and nearly 1 between atoms, which describes a negative corrugation. Both functions are displayed in Fig. 2 in gray-level form.

The first term in Eq. (3) represents the uncorrugated tunneling current, which decays much more slowly than the cor-

rugated terms. Therefore, if D_0 is not too small, the corrugation of the topographic image is

$$\Delta z = [(3\kappa_1^2/2\kappa^2 - \tfrac{1}{2})^2 - \tfrac{3}{2}|D_1/D_0|^2(k_1\kappa_1/\kappa^2)^2 - \tfrac{3}{8}|D_2/D_0|^2(k_1/\kappa)^4]\Delta z_0, \quad (5)$$

where

$$\Delta z_0 = (9/2\kappa)|B_1/B_0|^2 e^{-2(\kappa_1-\kappa)z}\phi^{(6)}(k\mathbf{x}) \quad (6)$$

is the corrugation of the Fermi-level LDOS of the sample. The ratio $|B_1/B_0|$ is determined by first-principles calculations or independent experimental measurements, such as helium-atom scattering.

In the following, we present numerical results for Au(111). Using the following parameters [4], $a=2.87$ Å, $k_1=1.46$ Å^{-1}, $\kappa=0.96$ Å^{-1}, and $\kappa_1=1.74$ Å^{-1}, we obtain

$$\Delta z = [19.6 - 11.4|D_1/D_0|^2 - 2.0|D_2/D_0|^2]\Delta z_0. \quad (7)$$

The enhancement factor E, i.e., the quantity in the square brackets of Eq. (7), is displayed in Fig. 3. Because the corrugation amplitude depends only on the relative intensities of different components, we normalize it through

$$|D_0|^2 + |D_1|^2 + |D_2|^2 = 1. \quad (8)$$

Naturally, the results can be represented by a diagram similar to a three-component phase diagram, as shown in Fig. 3. Several interesting features are worth noting. First, when the $m=0$ or d_{z^2} state dominates, a large, positive enhancement is expected. The condition for a substantial enhancement is quite broad. For example, when the condition $|D_0|^2 > 1.2|D_1|^2 + 0.2|D_2|^2$ is satisfied, the positive enhancement should be greater than 10, or a full order of magnitude. It is about 15% of the total phase space. To have an enhancement of more than 5, one-third of the total phase space is available. Therefore, the experimental observation of large positive corrugation enhancement should be frequent. Second, when $m\neq 0$ states dominate, an inverted corrugation should be observed. Again, the probability for a negative image to occur is large. Actually, when the condition $|D_0|^2 < 0.58|D_1|^2 + 0.1|D_2|^2$ is fulfilled, the image corrugation is inverted. This is about 43% of the total phase space. To have negative corrugations with an enhancement factor of 5 or more, 14% of the total phase space is available. Third, from Eq. (7) and Fig. 3, it is apparent that the effect of $m=1$ states in generating inverted corrugation is much stronger than that of $m=2$ states. This is expected from Figs. 1(c) and 1(d). The $m=1$ states have a much sharper rim than the $m=2$ states. Finally, there is a small region in which an almost complete cancellation of the positive enhancement and the negative enhancement can occur, as indicated by the shaded area near zero corrugation. In this case, the image is similar to the prediction of the s-wave model. The observed image corrugation in this case should be equal to or smaller than the corrugation of the Fermi-level LDOS. From Eq. (7) or Fig. 3, the available phase space is about 2.8% of the total phase space. Therefore, the probability is small. Practically, when this situation occurs, an almost flat image is observed. The experimentalist explains it as a bad tip. A tip sharpening procedure is then conducted until a large corrugation is observed, which is explained as having a good tip [1,4,6].

The corrugation inversion due to $m\neq 0$ tip states is a universal phenomenon in the STM imaging of low-Miller-index metal surfaces. For most metals (except several alkali and alkali earth metals, which have rarely been imaged by STM), the nearest-neighbor atomic distance $a \simeq 3$ Å. Consequently, the numerical coefficients in Eq. (7) are very close to those for Au(111). On the other hand, for profiles of reconstructions, the periodicity a can be much larger than 3 Å. For sufficiently large a, $\kappa_1/\kappa \to 1$, and $k_1/\kappa \to 0$. The STM images of such large reconstructions approach the result of the s-wave tip-state theory [10]. This limit case is demonstrated in the same experiment: As the atomic corrugation depends dramati-

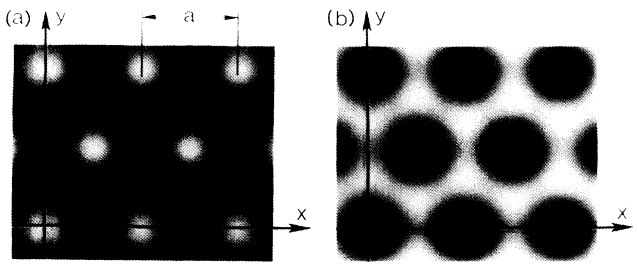

FIG. 2. Gray-scale representations of the hexagonal cosine function. Black represents 0, white represents 1. (a) The function $\phi^{(6)}(k\mathbf{x})$. (b) The function $1-\phi^{(6)}(k\mathbf{x})$.

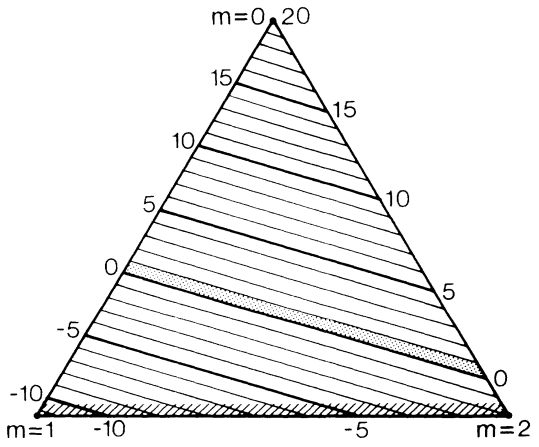

FIG. 3. Enhancement factor E for different d states at the tip apex. The shaded area near $E=0$ is the area where the s-wave tip state theory is valid. In the hatched area near the bottom, the theoretical amplitude of the negative corrugation shows a spurious divergence. See text.

cally on tip states, the average contour of the reconstruction in the $[1\bar{1}0]$ direction (with periodicity 63 Å) does not [4]. Consider its second harmonics, which represent the details of the reconstruction contour. The charge density is proportional to $|\psi|^2$, whose 31.5-Å-periodicity corrugation is determined by the fundamental Fourier component of a Bloch wave of periodicity 63 Å. The relevant parameters are $k_1 \simeq 2\pi/(63\ \text{Å}) \simeq 0.1\ \text{Å}^{-1}$ and $\kappa_1 = [0.96^2 + 0.1^2]^{1/2} \simeq 0.965$ Å. Substituting these numbers into Eq. (5), we obtain

$$\Delta z = [1.03 - 0.016|D_1/D_0|^2 - 4.4\times 10^{-5}|D_2/D_0|^2]Ce^{-0.01z}\cos^2(0.1x), \quad (9)$$

where C is the peak-to-peak amplitude of the second harmonics in the reconstruction contour.

From Eq. (9), it is clear that in the STM image of the $22\times\sqrt{3}$ reconstruction, the average contour (with the atomic corrugation neglected) is almost exactly the Fermi-level LDOS contour. In fact, for the contour of the reconstruction, the d_{z^2} tip state behaves almost exactly like an s state, and the effects of the $m\neq 0$ tip states are negligible. This verifies the conclusion of Tersoff and Hamann [10] that the STM topographic images of large superstructures of metal surfaces at low bias follow the Fermi-level LDOS contours, independent of tip states.

Now, we consider two alternative explanations. First, there is the possibility of explaining the negative corrugation by a ring of tip atoms; each has an s-wave state. Although a negative image can be constructed with certain choice of tip structures, the corrugation *amplitudes* of those images must not exceed the amplitudes for an s-wave tip state. It is too small to be observable. Second, Lang showed that when a nonmetal atom (such as He or O) is absorbed on a jellium surface, the Fermi-level LDOS at the atomic site appears as a minimum [12,13]. This phenomenon was observed by Kopatzki and Behm, where a depression near an oxygen atom was observed on the Ni(100) surface [14]. If the tip is an oxygen atom adsorbed on a metal surface, an image reversal is expected. Practically, the tunneling current goes through the metal atoms surrounding the oxygen atom. The configuration of those atoms is similar to the case of a ring of metal atoms as the tip. It is also too small to be observable.

In the derivation of Eq. (5), we assumed that the first term in Eq. (3) is not small. If the first term in Eq. (3) is very small, the corrugation amplitude can be obtained numerically. In this case, the negative corrugation amplitudes due to the $m\neq 0$ tip states are larger than the values given in Eq. (7). The enhancement for the negative corrugation is even larger than the values in Fig. 3. This situation can happen when $|D_0|^2$ is much smaller than $|D_1|^2$ or $|D_2|^2$ (as shown by the hatched area in Fig. 3). Mathematically, the corrugation amplitude diverges as a logarithmic singularity of the ratio $|D_1/D_0|^2$. Such a logarithmic divergence is similar to that of the anomalous-corrugation model for graphite images [15]. The corrugation enhancement in that case is extremely sensitive to a very small amount of tip states with a different m. According to the analysis of Tersoff and Lang, such an enhancement mechanism is not realistic for practical tips [16].

Using the same method presented here, it is easy to show that when an s state or a p_z state dominates the tip electronic states, corrugation inversion is unlikely to happen. The p_x and p_y states will cause corrugation inversion.

In conclusion, when an $m\neq 0$ state dominates the tip state near the Fermi level, the atomic corrugation of the STM image can be inverted. The amplitude of such inverted corrugation can be 1 order of magnitude larger than the corrugation amplitude of the Fermi-level LDOS contour of the sample surface. This phenomenon should be observed on low-Miller-index metal surfaces with nearest-neighbor atomic distances $a \simeq 3$ Å, which provides a quantitative explanation of the STM images with inverted atomic corrugations observed on metal surfaces.

The author wishes to acknowledge J. V. Barth and F. Gautier for helpful discussions and for communicating unpublished results.

[1] R. J. Behm, in *Scanning Tunneling Microscopy and Related Methods*, edited by R. J. Behm, N. Garcia, and H. Rohrer (Kluwer Academic, Dordrecht, 1990), pp. 173–210.
[2] S. Ciraci, A. Baratoff, and I. P. Batra, Phys. Rev. B **41**, 2763 (1990); **42**, 7618 (1990).
[3] G. Doyen, E. Kötter, J. P. Vigneron, and M. Scheffler, Appl. Phys. A **51**, 281 (1990).
[4] J. V. Barth, H. Brune, G. Ertl, and R. J. Behm, Phys. Rev. B **42**, 9307 (1990).
[5] C. J. Chen, Phys. Rev. Lett. **65**, 448 (1990).
[6] V. M. Hallmark, S. Chiang, J. F. Rabolt, J. D. Swalen, and R. J. Wilson, Phys. Rev. Lett. **59**, 2879 (1987); Ch. Wöll, S. Chiang, R. J. Wilson, and P. H. Lippel, Phys. Rev. B **39**, 7988 (1989); J. Wintterlin, J. Wiechers, H. Burne, T. Gritsch, H. Höfer, and R. J. Behm, Phys. Rev. Lett. **62**, 59 (1989).
[7] L. F. Mattheiss and D. R. Hamann, Phys. Rev. B **29**, 5372 (1984).
[8] S.-L. Weng, E. W. Plummer, and T. Gustafsson, Phys. Rev. B **18**, 1718 (1978); M. Posternak, H. Krakauer, A. J. Freeman, and D. D. Koelling, Phys. Rev. B **21**, 5601 (1980).
[9] S. Ohnishi and M. Tsukuda, Solid State Commun. **71**, 391 (1989).
[10] J. Tersoff and D. R. Hamann, Phys. Rev. B **31**, 805 (1985).
[11] C. J. Chen, Phys. Rev. B **42**, 8841 (1990).
[12] N. D. Lang, Phys. Rev. Lett. **56**, 1164 (1986).
[13] N. D. Lang, Comments Condensed Matter Phys. **14**, 253 (1989).
[14] E. Kopatzki and R. J. Behm, Surf. Sci. **245**, 255 (1991).
[15] J. Tersoff, Phys. Rev. Lett. **57**, 440 (1986).
[16] J. Tersoff and N. D. Lang, Phys. Rev. Lett. **65**, 1132 (1990).

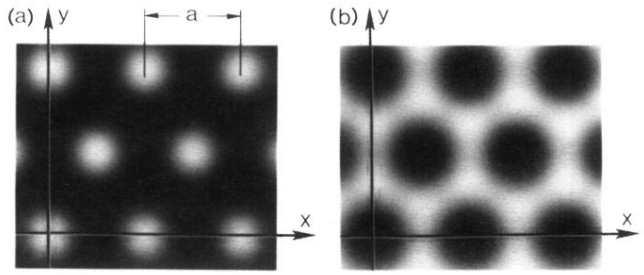

FIG. 2. Gray-scale representations of the hexagonal cosine function. Black represents 0, white represents 1. (a) The function $\phi^{(6)}(k\mathbf{x})$. (b) The function $1-\phi^{(6)}(k\mathbf{x})$.

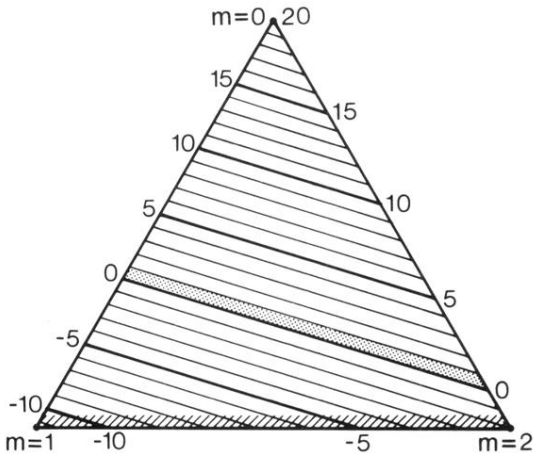

FIG. 3. Enhancement factor E for different d states at the tip apex. The shaded area near $E=0$ is the area where the s-wave tip state theory is valid. In the hatched area near the bottom, the theoretical amplitude of the negative corrugation shows a spurious divergence. See text.